

## MODELING OF ICE-SHEDDING FROM ACSR POWER LINE

HRABOVSKÝ Juraj<sup>1</sup>, GOGOLA Roman<sup>1</sup>, MURÍN Justín<sup>1</sup>, SEDLÁR Tibor<sup>1</sup>

<sup>1</sup>Slovak University of Technology in Bratislava, Faculty of Electrical Engineering and Information Technology,  
Department of Applied Mechanics and Mechatronics, Ilkovičova 3, 812 19 Bratislava, Slovakia  
e-mail: juraj.hrabovsky@stuba.sk

**Abstract:** In this contribution, the analysis of ice-shedding from Aluminium Conductor Steel Reinforced (ACSR) power lines is presented. The impact of the icing position on the overhead power lines, the resulting jump height, and impact on attachment tension points after ice-shedding is examined. In the numerical simulations the effective material properties of the ACSR conductor is calculated using the homogenisation method. Numerical analysis of one power line and double-bundle power lines with icing over the whole range or only on certain sections of single and double-bundle power lines are performed.

**KEYWORDS:** ACSR power line, ice-shedding, finite element method, transient analysis

### 1 Introduction

In cold regions, atmospheric icing is one of the major external loads threatening the reliability and mechanical integrity of overhead power lines. Ice-shedding from an iced overhead power line (eq. temperature rise) cause a vertical jump of the power lines and may lead to flashover if the phase-to-phase or phase-to-tower distance is smaller than the tolerable insulation distance. Therefore, it is necessary to determine the maximum jump height of an overhead power line after ice-shedding and to provide a reference for the design of the overhead power lines [1]. Ice-shedding can also cause dangerous vibrations in power lines, which can result in mechanical damage of the power line and power line pylons. Therefore, the transient analysis of ice-shedding is necessary.

Ice-shedding has been investigated with experimental, numerical and theoretical methods by many authors. Very approximate practical models have been suggested as early as the 1940s [2]. With the improvement of computational mechanics, numerical simulation methods (over all the finite element method - FEM) were used to study ice-shedding from the power lines eq. in [3] the simulation of the dynamic responses of transmission lines with different parameters after ice-shedding by means of FEM. In [4, 5] the dynamic behavior of bundle conductors and five-span line section after ice-shedding is numerically simulated. In [1], a new theoretical method to calculate the jump height of the overhead power line after ice-shedding is presented.

In this paper, the results of the transient analyses of ice-shedding from the ACSR power lines are presented. The results are calculated using a commercial finite element software ANSYS.

### 2 Modelling of ACSR power line

Aluminium Conductor Steel Reinforced (ACSR) cable are multi-wire conductors commonly used in overhead power lines. The outer strands of ACSR are made of aluminium due to its excellent conductivity, low weight and low cost. The center strands are made of steel for the strength required to support the weight without stretching the aluminium due to its ductility.

This gives the power lines an overall high tensile strength. So, the material of the ACSR conductor is inhomogeneous (Fig. 1) and it is complicated to model as a real conductor. Therefore, simplified models obtained by the homogenization of material properties are used.

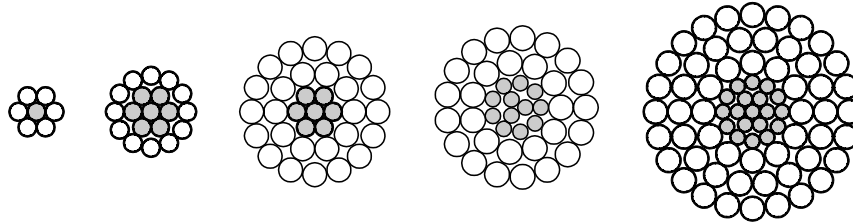


Fig. 1 Heterogeneous cross-section of the used ACSR conductor

Methods based on homogenization theory (e.g. the mixture rules [6]; self-consistent methods [7]) have been designed and successfully applied to determine the effective material properties of heterogeneous materials from the corresponding material behaviour of the constituents (and of the interfaces between them) and from the geometrical arrangement of the phases. In this context, the microstructure of the material under consideration is basically taken into account by the Representative Volume Element (RVE).

The homogenization techniques derived at our department for modelling Functionally Graded Material (FGM) [8, 9] can also be used for homogenization of the ACSR power lines. In case of the power line, the material properties vary layer-wise in the radial direction. The effective elasticity moduli for axial, shear, flexural and torsional loading are calculated from the condition, that the relevant stiffness of the cross-section compared with real construction (Fig. 2) is equal to the stiffness of the homogenized cross-section.

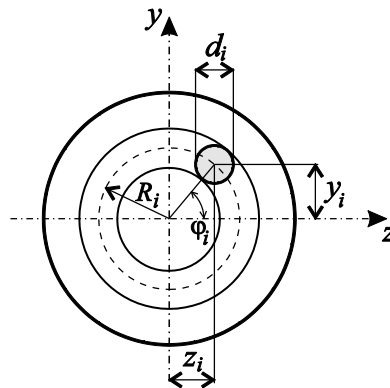


Fig. 2 Conductor cross-section

The real cross-section parameters of ACSR conductors are:  $R_i$  is the pitch circle,  $d_i$  is the wire diameter,  $\varphi_i$  is the angle of circumferential position of the wire,  $z_i$  and  $y_i$  are the position of the wire from the centre of the power line cross-section. The position of each wire can be calculated as follows:

$$y_i = R_i \sin \varphi_i \quad (1)$$

$$z_i = R_i \cos \varphi_i \quad (2)$$

Then the quadratic moment of the  $i^{\text{th}}$  wire cross-sectional area  $A_i = \pi d_i^2 / 4$  according to the  $y$  axis. With respect to the  $z$  axis the position can be calculated by equations [8, 10]:

$$I_{y_i} = \frac{\pi d_i^4}{64} + z_i^2 \frac{\pi d_i^2}{4} \quad I_{z_i} = \frac{\pi d_i^4}{64} + y_i^2 \frac{\pi d_i^2}{4} \quad (3)$$

The polar moment of the wire cross-sectional area to the origin of the coordinate system  $x, y$  is:

$$I_{\rho i} = I_{y_i} + I_{z_i} \quad (4)$$

We assume that the maximal and minimal elasticity modulus for lateral and transversal bending can be calculated by equations [8, 11]:

$$E_{L_{\max}}^{M_y H} = E_{L_{\max}}^{M_z H} = \frac{\sum_{i=1}^n E_i I_{y_i}}{\sum_{i=1}^n I_{y_i}} \quad (5)$$

$$E_{L_{\min}}^{M_y H} = E_{L_{\min}}^{M_z H} = \frac{\pi}{64} \left[ n_{Fe} d_{Fe}^2 E_{Fe} + n_{Al} d_{Al}^2 E_{Al} \right] \quad (6)$$

where  $n_{Fe}$  is the number of steel wires and  $n_{Al}$  is the number of aluminium wires. The maximal elasticity modulus represents the case, when all the wires are fixed together (e.g. after several years of lifetime), and the minimal elasticity modulus represents the case, when wires can slide over each other. In practice the effective elasticity modulus for lateral and transversal bending is assumed as the average value for maximal and minimal elasticity moduli [11]:

$$E_L^{M_y H} = \frac{E_{L_{\max}}^{M_y H} + E_{L_{\min}}^{M_y H}}{2} \quad (7)$$

$$E_L^{M_z H} = \frac{E_{L_{\max}}^{M_z H} + E_{L_{\min}}^{M_z H}}{2} \quad (8)$$

We also assume that the effective Poisson ratio is equal to [8]:

$$\nu_L^{NH} = \frac{\sum_{i=1}^n \nu_i A_i}{\sum_{i=1}^n A_i} \quad (9)$$

where  $\nu_i$  [-] is the Poisson ratio of the  $i^{th}$  wire. The effective mass density for axial beam vibration is [4]:

$$\rho_L^{NH} = \frac{\sum_{i=1}^n \rho_i A_i k_i}{A} \quad (10)$$

where  $\rho_i$  [kgm<sup>-3</sup>] is the material density of each wire and  $k_i$  [%] is the weight of each material increment due to stranding.

### 3 Icing and ice-shedding from power lines

Accumulating of ice on power lines is a very frequently problem for transmission systems situated in cold regions. Icing can also cause mechanical damage of the power lines because the tension in power lines can increase beyond its intended limits. In practice, the designers of power line transmission systems calculate the tension in power lines using a state equation [12] which includes the design icing loads for the area to which the designed power transmission

system is proposed (Tab. 1). At first, the reference icing load  $I_R$  [ $\text{Nm}^{-1}$ ] to unit length of the power line with diameter  $d$  [mm] is calculated using the equations shown in Tab. 1.

Tab.1 Calculation of the reference icing load  $I_R$  [ $\text{Nm}^{-1}$ ] [12]

Icing area	Reference icing load $I_R$ [ $\text{Nm}^{-1}$ ]
	$d \leq 30$ mm
N0	$1.298 + 0.1562d$
N1	$3.873 + 0.2698d$
N2	$10.566 + 0.4457d$
N3	$18.305 + 0.5866d$
N5	$35.376 + 0.8155d$
N8	$63.077 + 1.0890d$
N12	$102.063 + 1.3852d$
N18	$162.924 + 1.7501d$
NK	It is determined on a case by case

The nominal design icing load  $I_D$  is calculated using the formula [11]:

$$I_D = K_h I_R \gamma_I \quad (11)$$

where  $K_h$  [-] is the height factor of the icing load,  $\gamma_I$  [-] is the partial icing load factor. In the calculations of the mechanical stresses, it is needed to calculate the weather load factor  $z$  [-] (include icing), which is calculated using equation [11]:

$$z = \frac{q_1 + I_D}{q_1} \quad (12)$$

where  $q_1$  [ $\text{Nm}^{-1}$ ] is the gravity load of the power line. In practice, calculations mainly utilize the icing area in N2, so in simulating ice-shedding the icing load is calculated for this case.

When the ice formed on the power line drops off due to changing weather conditions (temperature, wind) or man-made shocks, it can cause ice-shedding (Fig. 3). The resulting drop causes the power line to swing upward. According to Fig. 3 it holds:

$$\Delta y = y_{mz} - y_{max} \quad (13)$$

where  $y_{max}$  [m] and  $y_{mz}$  [m] are maximal deflection with and without icing, respectively. The maximal jump height  $y_{sh}$  [m] of the power lines can be calculated as [11]:

$$y_{sh} = 2\Delta y \quad (14)$$

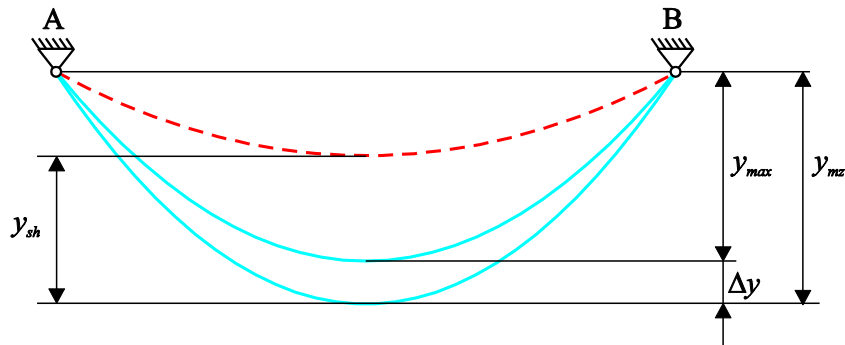


Fig. 3 Ice-shedding from power line

Ice-shedding causes vertical jump of the power line and may lead to flashover or can cause vibrations with high amplitudes and high forces within power lines (high forces at points of attachment). That is the reason, why it is necessary to determine the maximal power lines jump and resulting tensions. The analytical solution is available only for simple (symmetric) models [11]. Evaluation of these problems requires numerical simulation models using nonlinear analyses.

#### 4 Numerical experiment

Transient analyses of the single and double-bundle power lines according to Fig. 4 have been considered in this article. The symmetric conductor indicated as AlFe 445/74 (Fig. 4b) with a span length of  $L = 300$  m is used. The maximal deflection (without icing and for ambient temperature  $T_{amb} = 0$  °C) of the power line [11] is  $y_A = 7.73$  m.

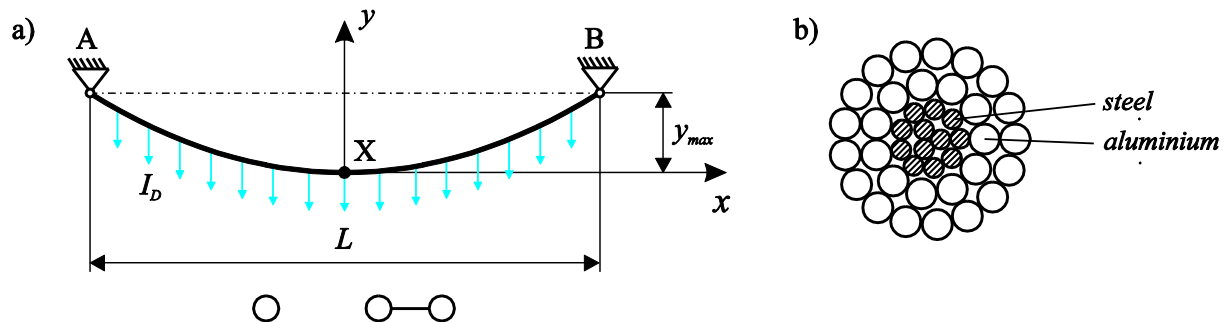


Fig. 4 The model of overhead power line with icing

The diameter of the aluminium wires is  $d_{Al} = 4.5$  mm and the diameter of the steel wires is  $d_{Fe} = 2.8$  mm. The effective cross-sections of the conducting parts are:  $A_{Fe} = 73.89$  mm<sup>2</sup>,  $A_{Al} = 445.32$  mm<sup>2</sup> and the effective cross-sectional area of the conductor is  $A = 519.21$  mm<sup>2</sup>.

Material properties of the material from which the power line is made of are [13, 14]:

- Steel:
  - Young's modulus:  $E_{Fe} = 207000$  MPa
  - Poisson's ratio:  $\nu_{Fe} = 0.28$
  - material density:  $\rho_{Fe} = 7780$  kgm<sup>-3</sup>
- Aluminium:
  - Young's modulus:  $E_{Al} = 69000$  MPa
  - Poisson's ratio:  $\nu_{Al} = 0.33$
  - material density:  $\rho_{Al} = 2703$  kgm<sup>-3</sup>

The guaranteed tensile strength of the conductor AlFe 445/74 is  $F_g = 139950$  N. Material properties for spacer dampers are: Young's modulus  $E_{SD} = 75000$  MPa, Poisson's ratio  $\nu_{SD} = 0.33$  and material density  $\rho_{SD} = 2730$  kgm<sup>-3</sup>.

The effective quadratic moments of the conductor cross-sectional area are:  $I_z = I_y = 28528.3 \text{ mm}^4$ . The effective circular cross-section of the conductor is constant with diameter  $d_{ef} = 25.71 \text{ mm}$  and the deformed length of the power line is  $L_d = 301.20 \text{ m}$ . The nominal design icing load is  $I_D = 23.83 \text{ Nm}^{-1}$  for the N2 icing area [11]. The effective material properties of the power line are:

$$E_L^{M,y,H} = E_L^{M,z,H} = 47929.78 \text{ MPa}$$

$$\nu_L^{NH} = 0.323$$

$$\rho_L^{NH} = 3482.81 \text{ kgm}^{-3}$$

These calculated effective material properties have been used in the transient analyses of the single and double-bundle power lines. Transient analyses of the ice-shedding of a single power line have been done utilizing a mesh of 1200 BEAM188 elements in the FEM program ANSYS [15]. Double-bundle power lines are connected with five spacer dampers distributed over 50 meters. The transient analyses of ice-shedding of the double-bundle power line with spacer dampers have been done with a mesh of 2415 BEAM188 elements.

Different ranges for the ice-shedding are considered in numerical simulations. The maximum jump height and axial forces in the attachment points for different ranges of ice-shedding are compared.

The deflection and the axial forces increase with an increase of icing over the power line length. The changes in the deflection  $\Delta y$  compared to the state with no icing at the lowest point of the span (point X) and the maximal axial forces at the attachment on insulator (point B) dependant on the icing location are shown in Tab. 2.

Tab. 2: The change in deflection  $\Delta y$  and maximal axial forces at the attachment point dependant on the icing location

Icing location [m]	single power line	double-bundle power line	Single power line	double-bundle power line
	$\Delta y$ [m]	$\Delta y$ [m]	$N_{max}$ [N]	$N_{max}$ [N]
–	–	–	25975.7	25946.4
0 – 300	1.833	1.834	49229.9	49306.2
25 – 275	1.836	1.837	48387.4	48468.6
50 – 250	1.806	1.808	46162.9	46254.5
0 – 200	1.662	1.663	45764.6	45799,8
0 – 150	0.901	0.902	39003.5	39037.1

As we can see in Tab. 2, there are small differences between the results of axial forces and changes in deflection in single and double-bundle power line. The differences are caused by spacer dampers placed on the conductors.

After ice-shedding the power line swings up. The maximal jump height  $y_{sh}$  [m] of the power lines are different for every range of the icing on the power lines in span. The results of swing heights in single and double-bundle power lines are shown in Tab. 3. In the case of an asymmetrical position of icing (0 – 200 and 0 – 150 m) the point of maximal deflection is observed (point X in Fig. 4).

Tab. 3: The maximum jump height for single and double-bundle power line

Icing location [m]	single power line			double-bundle power line	
	analytical	numerical		numerical	
	$y_{sh}$ [m]	$y_{sh}$ [m]	$t$ [s]	$y_{sh}$ [m]	$t$ [s]
0 – 300	3.67	3.91	1.406	3.91	1.406
25 – 275	3.67	3.89	1.381	3.89	1.380
50 – 250	3.61	3.73	1.336	3.73	1.336
0 – 200	3.32	3.30	1.341	3.31	1.342
0 – 150	1.80	1.93	1.366	1.93	1.369

After ice-shedding the power line will undergo oscillating motion. This dynamic phenomenon is damped by naturally by the power line itself and the damping of the environment. The constants  $\alpha = 0.10249$  [-] and  $\beta = 0.0244$  [-] for the Rayleigh's damping were used and are calculated from the damping ratio used in [14]. Time dependency of a single power line after ice-shedding for different ranges of ice-shedding is shown in Fig. 5. Time dependency of axial forces at the attachment point (point B) for a single power line is shown in Fig. 6.

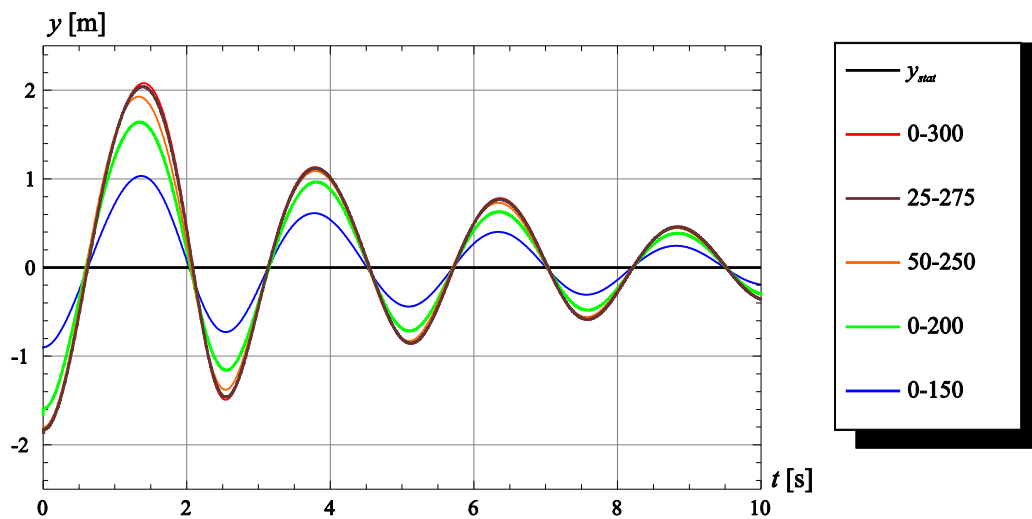


Fig. 5 Time dependency of single power line displacement after ice-shedding

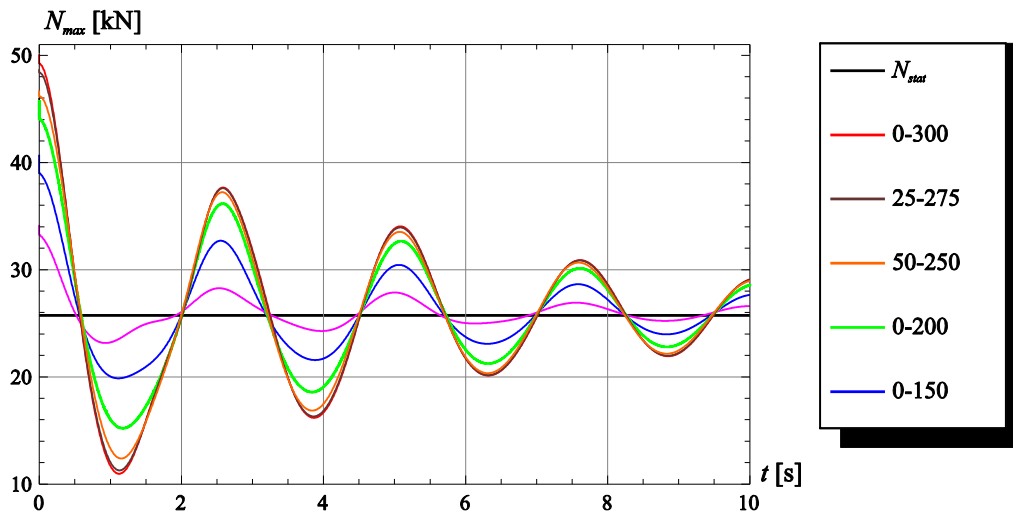


Fig. 6 Time dependency of axial forces at the attachment point (point B) for a single power line after ice-shedding

## 5 Conclusion

In this paper the FEM analysis of ice-shedding from overhead power lines - AlFe 445/74 (single and double-bundle) is presented using the commercial software ANSYS. The swing up height and axial forces in the attachment points for different ranges of ice-shedding have been evaluated and discussed.

From the numerical simulation is obvious that maximal axial forces at the attachment (on insulator) and the maximum jump heights of the power line after ice-shedding of partial icing are smaller than that in ice shedding over the entire span. It is also difficult to determine partial icing on the power line. Therefore, it is suitable to use extreme cases of ice-shedding over the entire span to assess jump height and axial forces at the attachment points of the power line after ice-shedding.

## ACKNOWLEDGEMENT

This work was supported by the Slovak Research and Development Agency under the contract No. APVV-0246-12 and APVV-14-0613, by Grant Agency VEGA, grant No. 1/0228/14 and 1/0453/15.

## REFERENCES

- [1] Chuan Wu, Bo Yana, Liang Zhang, Bo Zhang, Qing Li. A method to calculate jump height of iced transmission lines after ice-shedding. *Cold Regions Science and Technology*, **2016** (125), 40 – 47
- [2] VT. Morgan, DA. Swift Jump height of overhead-line conductors after the sudden release of ice loads. *Proc Inst Electr Eng* **1964** (111), 1736 – 1746.
- [3] M. Roshan Fekr, G. McClure. Numerical modelling of the dynamic response of ice-shedding on electric transmission lines, *Atmos. Res.*, **1998** (46), 1 – 11.
- [4] L.E. Kollár, M. Farzaneh Vibration of bundled conductors following ice shedding. *IEEE Trans. Power Delivery*, **2008**, (23), No. 2, 1097 – 1104.
- [5] L.E. Kollár, M. Farzaneh, P. Van Dyke. Modeling ice shedding propagation on transmission lines with or without interphase spacers. *IEEE Trans Power Apparatus Syst* **2013** (28), 261 – 267.

- [6] H. Altenbach, J. Altenbach, W. Kissing. Mechanics of composite structural elements. Springer Verlag, **2003**.
- [7] T. Reuter, G.J. Dvorak. Micromechanical models for graded composite materials: II. Thermomechanical loading. J. of the Mechanics and Physics of Solids, **1998** (46), 1655 - 1673.
- [8] J. Murín, V. Kutiš. Improved mixture rules for the composite (FGM's) sandwich beam finite element, Barcelona, Spain, **2007**, 647 - 650.
- [9] J. Murín, M. Aminbaghai, J. Hrabovský. Elastostatic Analysis of the Spatial FGM Structures. *Journal of Mechanical Engineering – Strojnícky časopis*, **2016** (65), No. 1, 27 - 56. doi: 10.1515/scjme-2016-0003
- [10] J. Murín, J. Hrabovský, R. Gogola, V. Goga, F. Janíček. Numerical Analysis and Experimental Verification of Eigenfrequencies of Overhead ACSR Conductor, *Transactions on Electrical Engineering*, **2016** (5), No. 4, 116 - 121.
- [11] Š. Fecko, D. Reváková, L. Varga, J. Lago, S. Ilenin. Vonkajšie elektrické vedenia, Bratislava, Renesans, s.r.o., **2010**.
- [12] M. Bindzár, Stavová rovnica - výpočet montážnych tabuliek, Bratislava, **2015**.
- [13] STN EN 50189, Vodiče na vonkajšie vedenia. Pozinkované oceľové drôty, **2001**.
- [14] STN EN 60889, Tvrdo ťahané hliníkové drôty pre vodiče nadzemných elektrických vedení, **2001**.
- [15] ANSYS Swanson Analysis System, Inc., „ANSYS Mechanical APDL Structural Analysis Guide,“ ANSYS, Houston.

